Sensors and Actuators B 185 (2013) 32–38

Contents lists available at SciVerse ScienceDirect

Sensors and Actuators B: Chemical

journal homepage: www.elsevier.com/locate/snb

Template-free synthesis of novel In_2O_3 nanostructures and their application to gas sensors

Xiumei Xu[a], Dawei Wang[a], Jing Liu[b], Peng Sun[a], Yue Guan[a], Heng Zhang[a], Yanfeng Sun[a], Fengmin Liu[a], Xishuang Liang[a], Yuan Gao[a], Geyu Lu[a,*]

[a] State Key Laboratory on Integrated Optoelectronics, College of Electronic Science and Engineering, Jilin University, 2699 Qianjin Street, Changchun 130012, China
[b] College of Information Science and Technology, Heilongjiang University, Harbin 150080, China

ARTICLE INFO

Article history:
Received 31 October 2012
Received in revised form 18 March 2013
Accepted 17 April 2013
Available online 26 April 2013

Keywords:
Indium oxide
Hydrothermal method
Novel
NO_2
Sensors

ABSTRACT

In this work, a novel flower-like indium hydroxide ($In(OH)_3$) structure was fabricated using a hydrothermal method, without any templates or surfactants. In_2O_3 with similar morphology was formed by annealing precursors $In(OH)_3$. The as-synthesized samples were characterized using X-ray powder diffraction (XRD), field emission scanning electron microscopy (FESEM), and transmission electron microscopy (TEM). The results indicate that the synthesized flower-like In_2O_3 were formed by porous nanosheets. Moreover, the gas sensing properties of as-prepared products were investigated. It was found that the sensor based on such novel In_2O_3 nanostructure exhibited high response and good selectivity to NO_2.

1. Introduction

Gas sensors have been widely researched for use in numerous applications [1–4]. Today, there has been extensive research on metal oxide semiconductor based gas sensors, such as SnO_2, ZnO, Fe_2O_3, WO_3, CuO, NiO [5–12], due to their industrial and domestic applications in toxic and flammable gas detection. Among them, indium oxide (In_2O_3) has been investigated extensively for its excellent gas sensing properties.

In_2O_3 is a very important wide-band-gap (direct band gap around 3.6 eV), *n*-type transparent semiconductor and has been widely used in microelectronic areas including window heaters, solar cells, liquid-crystal displays [13–17], and ultrasensitive gas sensors for detection of CO [18], O_3 [19], Cl_2 [20], CO [21], and NO_2 [22]. Many exciting results on In_2O_3 based gas sensors have been reported. Among most of the potential applications, the morphology and structure of the nanomaterials will undoubtedly play the pivotal role in determining their properties. In order to improve the performance of devices based on In_2O_3, various morphologies of In_2O_3 with different dimensional nanostructures, such as hollow microspheres, nanowires, nanobelts, nanotubes, nanocubes, nanofibers, nanosheets and complex hierarchical structures constructed with nanoscale building blocks [23–32], have been synthesized. Despite these advances, the unique morphologies of In_2O_3 spur researchers to explore their unknown properties and potential applications. Up to now, a variety of methods, including vapor–liquid–solid (VLS), solution–liquid–solid (SLS) phase catalytic growth, and anisotropic growth of crystalline nano-materials using proper capping agents have been introduced to fabricate nanostructures with the desired architectures. Another synthetic strategy is based on some templates, such as carbon nanotubes, porous alumina, mesoporous materials, polymers, surfactants, and biomolecules. These templates could physically confine the growth of nanostructures within the framework of the model. However, this template-assisted method is also restricted by the template materials. Subsequent removal of the template is tedious, and this postprocessing often destroys the desired product structure. Therefore, the development of template-free synthesis is seriously considered.

For this purpose, the synthesis of novel morphology In_2O_3 nanostructures through a facile, mild, and low cost method has been getting increasing attention. Herein, we report a facile method for the preparation of In_2O_3 hierarchical nanostructures by a hydrothermal process without using any surfactants or templates. Gas-sensing properties of the as prepared In_2O_3 products are also investigated. The as-obtained In_2O_3 novel nanostructures exhibited a high gas-sensing activity for NO_2, making them promising candidates for practical detectors for NO_2.

* Corresponding author. Tel.: +86 431 851 67808; fax: +86 431 851 67808.
E-mail addresses: syf@jlu.edu.cn (Y. Sun), lugy@jlu.edu.cn (G. Lu).

0925-4005/$ – see front matter
http://dx.doi.org/10.1016/j.snb.2013.04.078

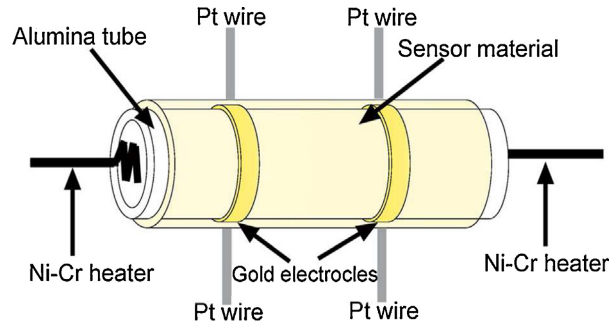

Fig. 1. Schematic structure of the gas sensor.

2. Experimental

2.1. Synthesis and characterization of In_2O_3

All the reagents (analytical-grade purity) were used without any further purification. In a typical synthesis, 0.381 g of $In(NO_3)_3 \cdot 4.5H_2O$ and 0.15 g urea were dissolved in 36 mL of deionized water with stirring for 60 min. Then, the mixture solution was transferred into a Teflon-lined stainless steel autoclave, sealed tightly, and maintained at 160 °C for 12 h. After the autoclave was cooled to room temperature naturally, the result product was washed with deionized water and absolute ethanol for several times using centrifuge, and then dried at 80 °C for 1 day. The products were loaded into an alumina boat, which was placed in a furnace. The furnace was slowly heated to 600 °C at a rate of 2 °C/min and then kept at 600 °C for 2 h. After the furnace was cooled to room temperature, the reaction products were collected.

X-ray power diffraction (XRD) analysis was conducted on a Rigaku D/max-2500 X-ray diffractometer with Cu $K\alpha_1$ radiation in the range of 20–70° (2θ) at a scanning rate of 6 °/min. The specific surface area was estimated using the Brunauer–Emmett–Teller (BET) equation based on the nitrogen adsorption isotherm obtained with a Micromeritics Gemini VII apparatus (Surface Area and Porosity System). Samples were degassed under vacuum at 200 °C for 4 h prior to the measurements. The pore size distribution was determined with the Barrett–Joyner–Halenda (BJH) method applied to the desorption branch of adsorption–desorption isotherm. Field emission scanning electron microscopy (FESEM) images were recorded on a JEOL JSM-7500F microscope operating at 15 kV. Transmission electron microscopy (TEM), selected-area electron diffraction (SAED), and high-resolution transmission electron microscopy (HRTEM) measurements were obtained on a JEOL JEM-2100 microscope operated at 200 kV.

2.2. Fabrication and measurement of sensor

Gas sensors were fabricated as follows: the as-prepared powder was mixed with the deionized water in order to make a paste, which was coated onto an alumina tube (4 mm in length, 1.2 mm in external diameter, and 0.8 mm in internal diameter, attached with a pair of gold electrodes) by a small brush to form a thick film. A pair of gold electrodes was installed at each end of the ceramic tube before it was coated with the paste; each electrode was connected with two Pt wire. A Ni–Cr heating wire was inserted into the tube to form an indirect-heated gas sensor. The structure of the sensor is shown in Fig. 1.

The gas-sensing properties of the samples were determined under laboratory conditions (50% ± 10% RH, 23 ± 1 °C). The gas-sensing properties of the samples were evaluated with a RQ-2 gas-sensing characterization system. The measurement was processed by a static process: a given amount of the tested gas was injected into a closed glass chamber, and the sensor was put into the chamber for the measurement of the sensitive performance. When the response reached a constant value, the upper cover of the test chamber was removed and the sensor began to recover in air. The response of the sensor was defined as $S = R_g/R_a$ for oxidizing gas or R_a/R_g for reducing gas, here, R_a and R_g were the resistances of the sensor in the air and target gas, respectively. The response and recovery times are defined as the time taken by the sensor to achieve 90% of the total resistance change in the case of adsorption and desorption, respectively.

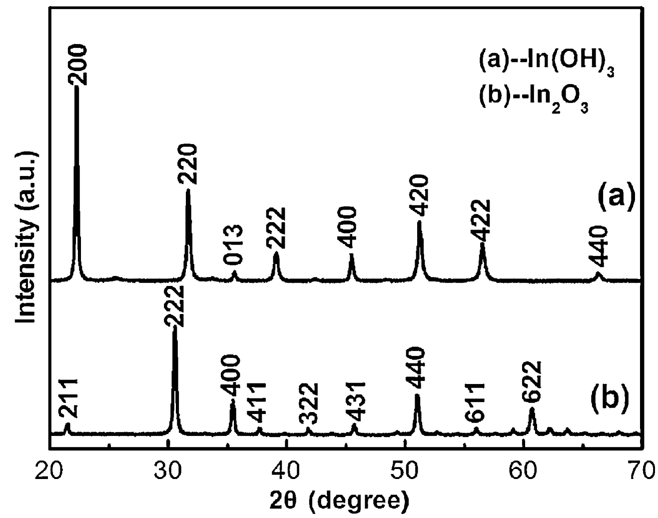

Fig. 2. X-ray diffraction patterns of as-prepared samples.

3. Results and discussion

3.1. Phase formation

X-ray powder diffraction (XRD) analysis was performed to investigate the crystal phases of the $In(OH)_3$ precursors prepared by hydrothermal method and the In_2O_3 products obtained by calcining the $In(OH)_3$ precursors. It can be seen from Fig. 2a that all the diffraction peaks could be very well indexed to the standard cubic $In(OH)_3$, which was consistent with the standard data file (JCPDS file No. 73-1810). After calcined at 600 °C, the $In(OH)_3$ precursors were converted into a pure cubic structure of In_2O_3 according to JCPDS card No. 06-416, with space group Ia-3 (No. 206) and lattice parameters of a = 10.118 Å. No diffraction peaks from any other impurities were observed, indicating the high purity of the products (Fig. 2b).

3.2. Structural and morphological characteristics

The morphology of the samples was investigated by field emission scanning electron microscopy (FESEM). Fig. 3 shows typical FESEM images of the $In(OH)_3$ and In_2O_3 samples at different magnifications. The low magnification FESEM image of $In(OH)_3$ (Fig. 3a) clearly reveals that the product is composed of hierarchical nanostructures with the size from 1 to 2 μm. No other morphologies could be detected, indicating a high yield of these structures. Fig. 3b shows the morphology of an individual flower-like structure at an enlarger-magnification FESEM, indicating that such structures are constructed from nano-sheets with irregular edges. After calcination at 600 °C, the obtained In_2O_3 samples retain the morphology and size of $In(OH)_3$ precursor, as shown in Fig. 3c. The detail morphology information can be found in Fig. 3d. It observed that the nanostructures are assembled by many irregular nanosheets with

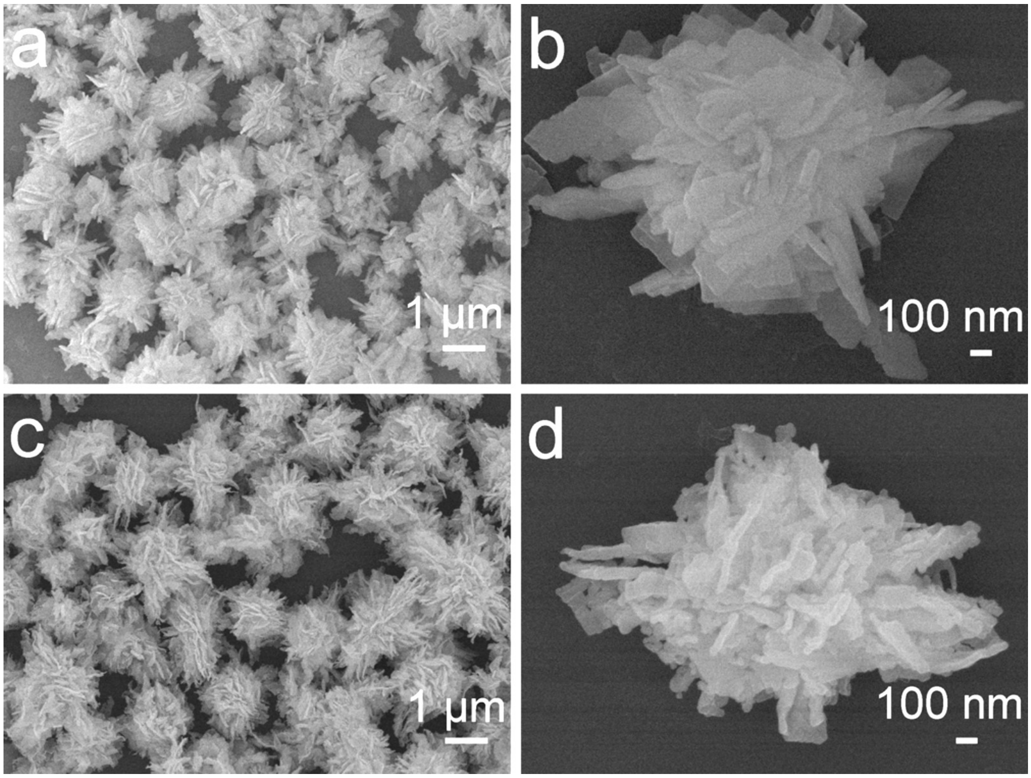

Fig. 3. Morphological characterization of as-synthesized samples: (a and b) $In(OH)_3$, (c and d) In_2O_3.

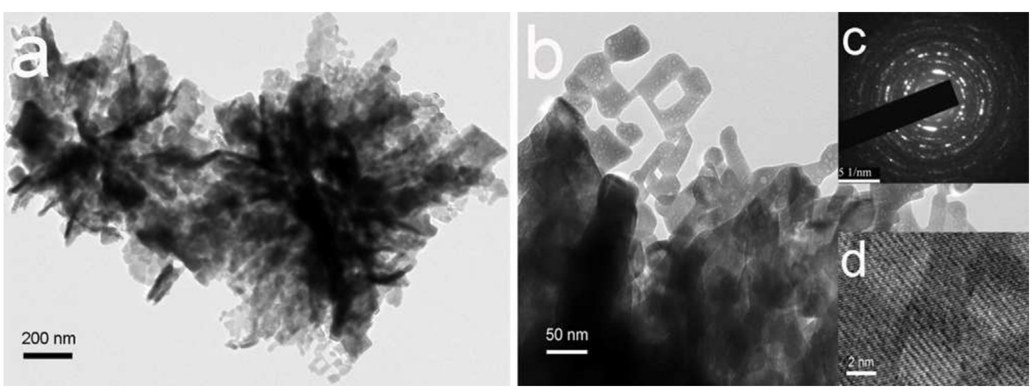

Fig. 4. Typical TEM images (a and b) of In_2O_3 nanostructures. The corresponding SAED (c) pattern. HRTEM images (d) taken from (a and b).

some small pores on them. This porous network is believed to be favorable for gas sensors, which can facilitate the inward and outward gas diffusion. The In_2O_3 flower-like structures are further characterized by TEM and HRTEM. As can be seen from Fig. 4a and b, In_2O_3 flower-like structures are obtained, which is in agreement with the SEM results (Fig. 3c and d). The corresponding SAED pattern (Fig. 4c) confirms that the porous In_2O_3 flower-like are polycrystalline structures in nature. The strong and sharp diffraction peaks in the XRD pattern and the clear lattice fringes in the HRTEM image (Fig. 4d) led us to believe that the flower-like nanostructure is In_2O_3.

To investigate the role of urea in the formation of hierarchical flower-like $In(OH)_3$, the controlled experiments of the hydrothermal process with different concentrations of urea had been carried out by keeping other experimental conditions constant. When the experiments were performed with adding 0.05 g urea, only irregular nanocubes were obtained (Fig. 5a). As shown in Fig. 5b, upon adding 0.15 g of urea, the obtained products consisted of flower-like hierarchical nanostructures. As the amount of urea was increased to 0.5 g, the product was the mixture of the flower-like structure and irregular nanosheets (Fig. 5c). The insets in (a), (b) and (c) are their corresponding high-magnification FESEM images, respectively. According to the above results, it can be concluded that urea plays an important role in forming $In(OH)_3$ flower-like nanostructures.

To further obtain the information about the as-prepared In_2O_3, the nitrogen adsorption and desorption measurements were performed at 77 K. The representative N_2 adsorption and desorption isotherm and the corresponding BJH pore size distribution plot (inset of Fig. 6) of the hierarchical microspheres are shown in Fig. 6. The BET surface area of the product was calculated to be 32.8 m^2/g with the Brunauer–Emmett–Teller (BET) method. The adsorption–desorption isotherms are typical type IV with a hysteresis loop according to the IUPAC classification, indicating that the powders contain disordered mesopores. Pore size distribution curves were calculated from the desorption branch of a nitrogen isotherm by the BJH method using the Halsey equation.

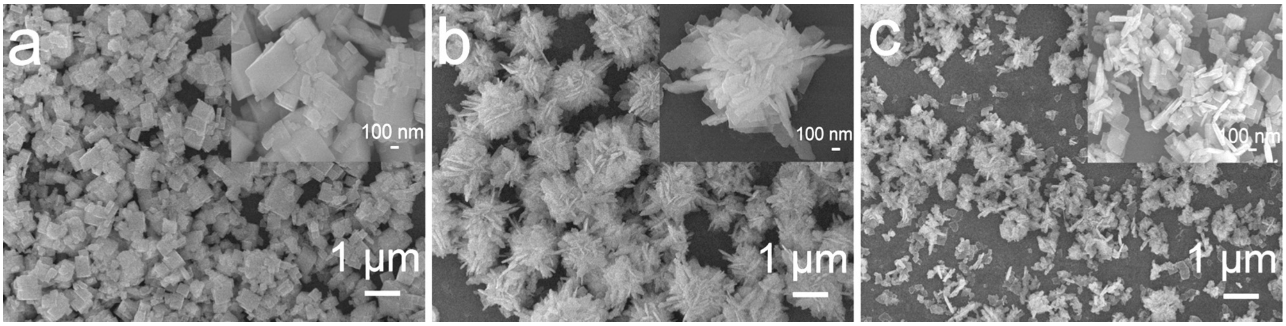

Fig. 5. FESEM images of $In(OH)_3$ products synthesized under hydrothermal reaction with the presence of different amounts of urea of (a) 0.05 g, (b) 0.15 g and (c) 0.5 g. The insets in (a), (b) and (c) are their corresponding high-magnification FESEM images, respectively.

3.3. Gas-sensing properties for NO_2

The gas sensing properties of the sensor using hierarchical In_2O_3 were investigated. It is well known that the response of a sensor is influenced by its operating temperature [22,33]. In order to determine an optimum operating temperature, the response of the sensor towards 50 ppb NO_2 was examined as a function of operating temperature. The correlation of the response and response time of the sensor based on flower-like In_2O_3 to 50 ppb NO_2 with the operating temperature was measured and shown in Fig. 7. It revealed that the response time decreases with increasing operating temperature. This tendency indicates that fast response can be obtained through increasing the operating temperature. However, when the operating temperature is too high, the gas response decreases sharply. The maximum response to NO_2 is about 19.4 at 125 °C. Therefore, optimal operating temperatures of 125 °C was chosen for sensor based on flower-like In_2O_3, to further examine the characteristics of gas sensors. To demonstrate the performance of the In_2O_3 as an excellent sensing material, the relationship between response and NO_2 concentrations for the sensor at operating temperature of 125 °C is depicted in Fig. 8. The resistance of the sensor increases upon exposure NO_2, whereas it decreases upon the removal of NO_2. Furthermore, the response of the sensor to NO_2 increased with the increasing of the NO_2 concentration. The response was about 3.9, 7.2, 10.1, 13.7 and 19.4 to 10, 20, 30, 40, 50 ppb NO_2, respectively. Specifically, the sensor using In_2O_3 was found to exhibit high responses to NO_2 even at low concentrations. When the sensor was exposed to 5 ppb NO_2, the response was 2.4. A comparison between the sensing performances of the sensor and literature reports [34–39] is summarized in Table 1. The advantage of our In_2O_3 sensors is a relatively higher response to NO_2, so it can be expected to serve as a promising functional material in NO_2 gas sensors. The response and recovery characteristics to 50 ppb NO_2 at operating temperature of 125 °C were investigated, and the curve is shown in Fig. 9. The results indicate that the flower-like In_2O_3 sensor had a fast response-recovery kinetics. The response and recovery times of the flower-like In_2O_3 sensor were about 100 and 30 s, respectively. Compared with the sensing properties of sensors using other In_2O_3 nanostructure [23,40–42], it could be seen that the flower-like In_2O_3 sensor had a relative shorter response and recovery times. Five reversible cycles of the response curve

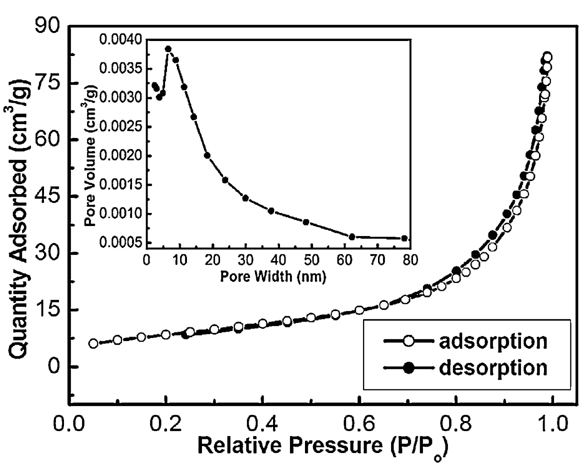

Fig. 6. Typical N_2 adsorption–desorption isotherms of In_2O_3 flower-like structures. The inset is the corresponding pore size distribution curve.

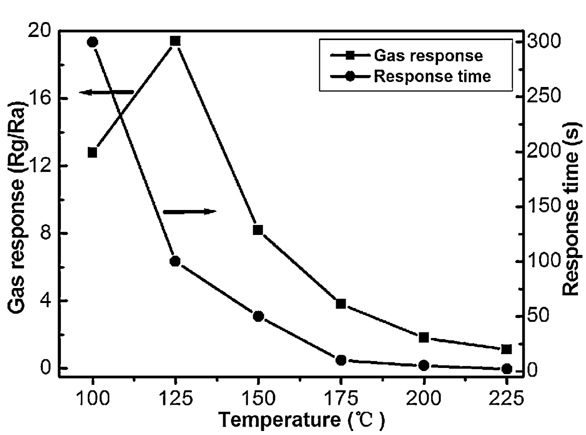

Fig. 7. Correlations between the gas response and response time to 50 ppb NO_2 and the operating temperature for the sensor using the as-prepared In_2O_3.

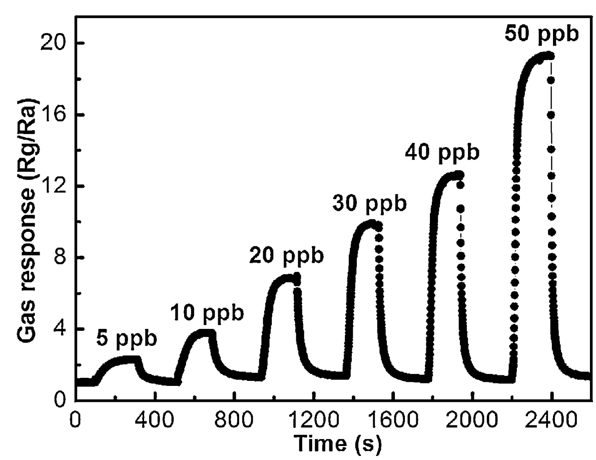

Fig. 8. Responses to different concentrations of NO_2 for the sensor using the flower-like In_2O_3 at 125 °C.

Table 1
Gas responses to NO_2 in the present study and those reported in the literatures [10,34–39].

Sensing materials	NO_2 concentration (ppm)	Operation temperature (°C)	Sensor response	Reference
In_2O_3 thin film	5	200	~10	[34]
In_2O_3 nanowires (using AAM)	10	150	56	[35]
WO_3 nanowire array	0.25	180	~3	[36]
WO_3 films	0.1	100	~18	[37]
WO_3 nanosheets	0.1	150	~7	[10]
ZnO nanowires	10	200	19.1	[38]
ZnO–SnO_2 NWs	10	200	66.3	[39]
In_2O_3 nanostructures	0.05	125	19.4	Present work

indicated that the sensor had good repeatability and stability, as shown in the inset of Fig. 9.

Since selectivity is an important parameter of gas sensors for its practical application, the selectivity of the sensor was measured. Fig. 10 shows the response of sensors using hierarchical In_2O_3 to various target gasses, such as NH_3, Cl_2, H_2S, CO, SO_2, CH_3CH_2OH and O_3. All of the gasses were tested at an operating temperature of 125 °C. We can see that this sensor shows the highest response to NO_2, while its response to 1 ppm O_3 is 17.4. The response of the sensor to Cl_2, and SO_2 is much lower, and the response to other gases or vapors such as CO, H_2S, NH_3, C_2H_5OH is negligible. The results indicated that the as-prepared hierarchical flower-like In_2O_3 nanostructures displayed superior selectivity to NO_2 against the other interference gasses and was very suitable for sensing NO_2 at 125 °C.

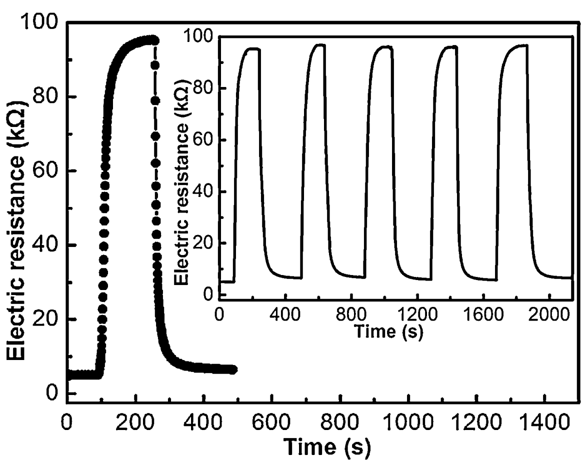

Fig. 9. Response transients of the sensor to 50 ppb NO_2 at 125 °C, the inset displaying five periods of response curve.

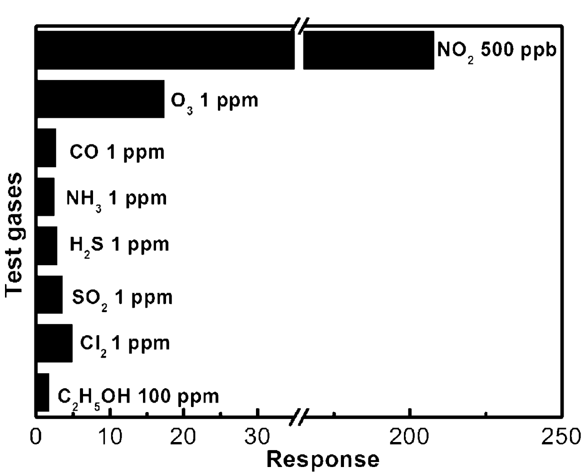

Fig. 10. Cross-responses of the sensor to various test gases at 125 °C.

When NO_2 is detected by In_2O_3 sensor, not only NO_2 adsorption and related In_2O_3 conductivity changes, but also the possibility of chemical interaction between indium oxide and NO_2 as well as stipulated change of defect concentration should be taken into account [22,35,43,44]. These chemisorbed oxygen ions (O_2^-, O^-, and O^{2-}) can induce an electron-depleted region on the surface of *n*-type In_2O_3, resulting in the increase in surface potential barrier [45,46]. When the sensor exposed to NO_2 gas at optimum temperature, the adsorbed NO_2 molecules on surface of In_2O_3 act as an electron acceptor (Eq. (1)).

$$NO_{2(gas)} + e^- \rightarrow NO_{2(ads)}{}^- \quad (1)$$

$$NO_{2(gas)} + O_{2(ads)}{}^- + 2e^- \rightarrow NO_{2(ads)}{}^- + 2O_{(ads)}{}^- \quad (2)$$

$$NO_{2(gas)} + O_{(ads)}{}^- \rightarrow NO_{(ads)}{}^+ + 2O_{(ads)}{}^- \quad (3)$$

This leads to a decrease in electron concentration at surface and correspondingly, the resistance of In_2O_3 nanostructures increases. As shown by Eqs. (2) and (3), the electrons, the electrons in the In_2O_3 are transferred to NO_2 or the absorbed oxygen in the reaction process, which explains the increase of the resistance under the NO_2 atmosphere. Yamazoe et al. [47] had reported that the stable response involves the gas diffusing to the sensing material, adsorption on the material, reaction with the material and then the conductivity changes of the material. The hierarchical structures of the obtained In_2O_3 samples provide well-defined and well-aligned micro-, and nanoporosity for effective gas diffusion. Therefore, the entire hierarchical nanostructures were quickly converted into a highly insulating state when exposed to the oxidizing gas. The quick resistance changes of the whole hierarchical nanostructures ensure the high gas response and fast response and recovery properties. In addition, the irregular nanosheets which consist of the hierarchical structure are full of pores on the surface. The abundant pores are also beneficial for the enhancement of gas response. So, a fast response/recovery property and high response can be achieved using as-synthesized sample.

4. Conclusion

In summary, flower-like In_2O_3 had been successfully synthesized through a simple hydrothermal process without any templates or surfactants, after calcining of precursor $In(OH)_3$ at 600 °C for 2 h. Field emission scanning electron microscopic and transmission electron microscopic results that the flower-like hierarchical architectures were composed of nanosheets with pore on them. In addition, the gas sensing properties of sensors based on as-synthesized In_2O_3 towards NO_2 were investigated. The sensor fabricated from these hierarchical structures exhibits excellent NO_2 sensing properties at relatively low operating temperature. The sensor response is about 2.4 to 5 ppb NO_2 at 125 °C. These results suggest that our sensor might have potential application to fabricate highly sensitive and low power consumption NO_2 gas sensor.

Acknowledgements

This work was supported by the National Nature Science Foundation of China (Nos. 61006055, 61074172, 61134010) and Program for Chang Jiang Scholars and Innovative Research Team in University (No. IRT1017).

References

[1] N. Barsan, D. Koziej, U. Weimar, Metal oxide-based gas sensor research: how to? Sensors and Actuators B: Chemical 121 (2007) 18–35.
[2] J. Tamaki, High sensitivity semiconductor gas sensors, Sensor Letters 3 (2005) 89–98.
[3] G. Korotcenkov, Metal oxides for solid-state gas sensors: what determines our choice, Materials Science and Engineering B: Solid State Materials for Advanced Technology 139 (2007) 1–23.
[4] N. Yamazoe, K. Shimanoe, New perspectives of gas sensor technology, Sensors and Actuators B: Chemical 138 (2009) 100–107.
[5] G.Y. Lu, J. Xu, J.B. Sun, Y.S. Yu, Y.Q. Zhang, F.M. Liu, UV-enhanced room temperature NO_2 sensor using ZnO nanorods modified with SnO_2 nanoparticles, Sensors and Actuators B: Chemical 162 (2012) 82–88.
[6] J. Tamaki, Y. Okochi, S. Konishi, Effect of oxide-electrode interface on dilute NO_2 sensing properties of WO_3 thin film nanosensors, Electrochemistry (Tokyo, Jpn.) 74 (2006) 159–162.
[7] L.P. Zhu, N.C. Bing, L.L. Wang, H.Y. Jin, G.H. Liao, L.J. Wang, Self-assembled 3D porous flowerlike α-Fe_2O_3 hierarchical nanostructures: synthesis, growth mechanism, and their application in photocatalysis, Dalton Transactions 41 (2012) 2959–2965.
[8] H.J. Zhang, R.F. Wu, Z.W. Chen, G. Liu, Z.N. Zhang, Z. Jiao, Self-assembly fabrication of 3D flower-like ZnO hierarchical nanostructures and their gas sensing properties, Crystal Engineering Communication 14 (2012) 1775–1782.
[9] F. Song, H.L. Su, J.J. Chen, W.J. Moon, W.M. Lau, D. Zhang, 3D hierarchical porous SnO_2 derived from self-assembled biological systems for superior gas sensing application, Journal of Materials Chemistry 22 (2012) 1121–1126.
[10] L. You, Y.F. Sun, J. Ma, Y. Guan, J.M. Sun, Y. Du, G.Y. Lu, Highly sensitive NO_2 sensor based on square-like tungsten oxide prepared with hydrothermal treatment, Sensors and Actuators B: Chemical 157 (2011) 401–407.
[11] J.P. Liu, X.T. Huang, Y.Y. Li, Z.K. Li, Q.B. Chi, G.Y. Li, Formation of hierarchical CuO microcabbages as stable bionic super hydrophobic materials via a room-temperature solution-immersion process, Solid State Sciences 11 (2008) 1568–1576.
[12] S.L. Xiong, C.Z. Yuan, X.G. Zhang, Y.T. Qian, Mesoporous NiO with various hierarchical nanostructures by quasi-nanotubes/nanowires/nanorods self-assembly: controllable preparation and application in supercapacitors, Crystal Engineering Communication 13 (2011) 626–632.
[13] D.H. Zhang, C. Li, S. Han, X.L. Liu, T. Tang, W. Jin, C.W. Zhou, Electronic transport studies of single-crystalline In_2O_3 nanowires, Applied Physics Letters 82 (2003) 112–114.
[14] C.G. Granqvist, Transparent conductive electrodes for electrochromic devices: a review, Applied Physics A: Solids and Surfaces 57 (1993) 19–24.
[15] Y. Shigesato, S. Takaki, T. Haranoh, Electrical and structural properties of low resistivity tin-doped indium oxide films, Journal of Applied Physics 71 (1992) 3356–3364.
[16] A. Gurlo, M. Ivanovskaya, N. Bârsan, M. Schweizer-Berberich, U. Weimar, W. Göpel, A. Diéguez, Grain size control in nanocrystalline In_2O_3 semiconductor gas sensors, Sensors and Actuators B: Chemical 44 (1997) 327–333.
[17] M. Liess, Electric-field-induced migration of chemisorbed gas molecules on a sensitive film-a new chemical sensor, Thin Solid Films 410 (2002) 183–187.
[18] Nandan Singh, Chaoyi Yan, Pooi See Lee, Room temperature CO gas sensing using Zn-doped In_2O_3 single nanowire field effect transistors, Sensors and Actuators B: Chemical 150 (2010) 19–24.
[19] G. Korotcenkova, A. Cerneavschia, V. Brinzaria, A. Vasilieva, M. Ivanova, A. Cornetb, J. Moranteb, A. Cabotb, J. Arbiolb, In_2O_3 films deposited by spray pyrolysis as a material for ozone gas sensors, Sensors and Actuators B: Chemical 99 (2004) 297–303.
[20] J. Tamaki, C. Naruo, Y. Yamamoto, M. Matsuoka, Sensing properties to dilute chlorine gas of indium oxide based thin film sensors prepared by electron beam evaporation, Sensors and Actuators B: Chemical 83 (2002) 190–194.
[21] Potentiometric sensor based on NASICON and In_2O_3 for detection of CO_2 at room temperature-modification with foreign substances, Sensors and Actuators B: Chemical 76 (2001) 639–643.
[22] T. Hyodo, H. Inoue, H. Motomur, K. Matsuo, T. Hashishin, J. Tamaki, Y. Shimizu, M. Egashira, NO_2 sensing properties of macroporous In_2O_3-based powders fabricated by utilizing ultrasonic spray pyrolysis employing polymethylmethacrylate microspheres as a template, Sensors and Actuators B: Chemical 151 (2010) 265–273.
[23] P.C. Xua, Z.X. Cheng, Q.Y. Pan, J.Q. Xu, Q. Xiang, W.J. Yu, Y.L. Chu, High aspect ratio In_2O_3 nanowires: synthesis, mechanism and NO_2 gas-sensing properties, Sensors and Actuators B: Chemical 130 (2008) 802–808.
[24] P. Guha, S. Kar, S. Chaudhuri, Direct synthesis of single crystalline In_2O_3 nanopyramids and nanocolumns and their photoluminescence properties, Applied Physics Letters 85 (2004) 3851–3853.
[25] Y.G. Yan, Y. Zhang, H.B. Zeng, L.D. Zhang, In_2O_3 nanotowers: controlled synthesis and mechanism analysis, Crystal Growth and Design 7 (2007) 940–943.
[26] C.H. Liang, G.W. Meng, Y. Lei, F. Phillipp, L.D. Zhang, Catalytic growth of semiconducting In_2O_3 nanofibers, Advanced Materials 13 (2001) 1330–1333.
[27] Z.X. Cheng, X.B. Dong, Q.Y. Pan, J.C. Zhang, X.W. Dong, Preparation and characterization of In_2O_3 nanorods, Materials Letters 60 (2006) 3137–3140.
[28] C. Li, D.H. Zhang, S. Han, X.L. Liu, T. Tang, C.W. Zhou, Diameter-controlled growth of single-crystalline In_2O_3 nanowires and their electronic properties, Advanced Materials 15 (2003) 143–146.
[29] Q.S. Liu, W.G. Lu, A.H. Ma, J.K. Tang, J. Lin, J.Y. Fang, Study of quasi-monodisperse In_2O_3 nanocrystals: synthesis and optical determination, Journal of the American Chemical Society 127 (2005) 5276–5277.
[30] C.Q. Wang, D. Chen, X.L. Jiao, C.L. Chen, Lotus-root-like In_2O_3 nanostructures: fabrication, characterization, and photoluminescence properties, Journal of Physical Chemistry C 111 (2007) 13398–13403.
[31] X.P. Shen, H.J. Liu, X. Fan, Y. Jiang, J.M. Hong, Construction and photoluminescence of In_2O_3 nanotube array by CVD-template method, Journal of Crystal Growth 276 (2005) 471–477.
[32] Y.F. Hao, G.W. Meng, C.H. Ye, L.D. Zhang, Controlled synthesis of In_2O_3 octahedrons and nanowires, Crystal Growth and Design 5 (2005) 1617–1621.
[33] A. Kolmakov, M. Moskovits, Chemical sensing and catalysis by one-dimensional metal-oxide nanostructures, Annual Review of Materials Research 34 (2004) 151–180.
[34] S. Bianchi, E. Comini, M. Ferroni, G. Faglia, A. Vomiero, G. Sberveglieri, Indium oxide quasi-monodimensional low temperature gas sensor, Sensors and Actuators B: Chemical 118 (2006) 204–207.
[35] C.S. Rout, K. Ganesh, A. Govindaraj, C.N.R. Rao, Sensors for the nitrogen oxides, NO_2, NO and N_2O, based on In_2O_3 and WO_3 nanowires, Applied Physics A 85 (2006) 241–246.
[36] B. Cao, J. Chen, X. Tang, W. Zhou, Growth of monoclinic WO_3 nanowire array for highly sensitive NO_2 detection, Journal of Materials Chemistry 19 (2009) 2323–2327.
[37] A. Ponzoni, E. Comini, M. Ferroni, G. Sberveglieri, Nanostructured WO_3 deposited by modified thermal evaporation for gas-sensing applications, Thin Solid Films 490 (2005) 81–85.
[38] S. Öztürk, N. Kılınç, N. Taşaltin, Z.Z. Öztürk, A comparative study on the NO_2 gas sensing properties of ZnO thin films, nanowires and nanorods, Thin Solid Films 520 (2011) 932–938.
[39] I. Hwang, S. Kim, J. Choi, J. Choi, H. Ji, G. Kim, G. Cao, J. Lee, Synthesis and gas sensing characteristics of highly crystalline ZnO–SnO_2 core-shell nanowires, Sensors and Actuators B: Chemical 148 (2010) 595–600.
[40] S.S. Kim, J.Y. Park, S.W. Choi, H.S. Kim, H.G. Na, J.C. Yang, H.W. Kim, Significant enhancement of the sensing characteristics of In_2O_3 nanowires by functionalization with Pt nanoparticles, Nanotechnology 21 (2010) 415502–415509.
[41] D. Zhang, Z. Liu, C. Li, T. Tang, X. Liu, S. Han, B. Lei, C. Zhou, Detection of NO_2 down to ppb levels using individual and multiple In_2O_3 nanowire devices, Nano Letters 4 (2004) 1919–1924.
[42] H. Steffes, C. Imawan, P. Fricke, H. Vöhse, J. Albrecht, R. Schneider, F. Solzbacher, E. Obermeier, New $In_xO_yN_z$ films for the application in NO_2 sensors, Sensors and Actuators B: Chemical 77 (2001) 352–358.
[43] L. Francioso, A. Forleo, S. Capone, M. Epifani, A.M. Taurino, P. Siciliano, Nanostructured In_2O_3–SnO_2 sol–gel thin film as material for NO_2 detection, Sensors and Actuators B: Chemical 114 (2006) 646–655.
[44] H. Steffes, C. Imawan, F. Solzbacher, E. Obermeier, Reactivity RF-sputtering In_2O_3 thin films for detection of NO_2, in: Proceedings of the International Conference Eurosensors XIII, The Hague, The Netherlands, 12–15 September, 1999, pp. 871–874.
[45] M. Epifani, J.D. Prades, E. Comini, E. Pellicer, M. Avella, P. Siciliano, G. Faglia, A. Cirera, R. Scotti, F. Morazzoni, J.R. Morante, The role of surface oxygen vacancies in the NO_2 sensing properties of SnO_2 nanocrystals, Journal of Physical Chemistry C 112 (2008) 19540–19546.
[46] H. Liu, J.X. Wan, Q.Y. Fu, M. Li, W. Luo, Z.Q. Zheng, H.F. Cao, Y.X. Hu, D.X. Zhou, Tin oxide films for nitrogen dioxide gas detection at low temperatures, Sensors and Actuators B: Chemical 177 (2013) 460–466.
[47] N. Yamazoe, G. Sakai, K. Shimanoe, Oxide semiconductor gas sensors, Catalysis Surveys from Asia 7 (2003) 63–75.

Biographies

Xiumei Xu received her BS degree from College of Chemistry, Liaocheng University, China in 2008. She entered the PhD course in 2011, majored in microelectronics and solid state electronics. Now, she is engaged in the synthesis and characterization of the semiconducting functional materials and gas sensors.

Dawei Wang received his BS degree in 2011 from Jilin University of China at the Electronics Information and Engineering department. He entered the MS course in 2011, majored in the design and fabrication of micro-hot plates.

Jing Liu received her MS degree in Software Institute of Software Engineering in 2008. Presently, she is a teacher in Information Science and Technology of Heilongjiang University.

Peng Sun received his MS degree from State Key Laboratory of Superhard Materials, Jilin University, China in 2009. He entered the PhD course in 2010, majored in microelectronics and solid state electronics. Now, he is engaged in the synthesis and characterization of the semiconducting functional materials and gas sensors.

Yue Guan received his BS degree from the Electronics Science and Engineering Department, Jilin University, China in 2009. Presently, he is a graduate student, majored in microelectronics and solid state electronics.

Heng Zhang entered the BS course in 2010, majored in electronic science and technology.

Yanfeng Sun obtained his PhD from Jilin University of China in 2007. Presently, he is working as associate professor in Electronics Science and Engineering Department of Jilin University. His current research interests are nanoscience and gas sensors.

Fengmin Liu received the BE degree in Department of Electronic Science and Technology in 2000. She received his Doctor's degree in College of Electronic Science and Engineering at Jilin University in 2005. Now she is an associate professor in Jilin University, China. Her current research is preparation and application of semiconductor oxide, especial in gas sensor and solar cell.

Xishuang Liang received the BE degree in Department of Electronic Science and Technology in 2004. He received his Doctor's degree in College of Electronic Science and Engineering at Jilin University in 2009. Now he is a lecturer of Jilin University, China. His current research is solid electrolyte gas sensor.

Yuan Gao received her Doctor's degree in Department of Analytical Chemistry at Jilin University in 2012. Now she is a lecturer in Jilin University, China. Her current research is preparation and application of graphene oxide and semiconductor oxide, especial in gas sensor and biosensor.

Geyu Lu received the BS degree in electronic sciences in 1985 and the MS degree in 1988 from Jilin University in China and the Dr Eng degree in 1998 from Kyushu University in Japan. Now he is a professor of Jilin University, China. Now, he is interested in the development of functional materials and chemical sensors.